Analysis of the Vibrational Behavior of dual-fuel RCCI combustion in a Heavy-Duty Compression Ignited Engine fueled with Diesel-NG at Low Load

Analysis of the Vibrational Behavior of dual-fuel RCCI combustion in a Heavy-Duty Compression Ignited Engine fueled with Diesel-NG at Low Load

Giacomo Silvagni*, Davide Moro*, Vittorio Ravaglioli*, Fabrizio Ponti*, Enrico Corti*, Alessandro Brusa*, Nicoló Cavina*, Abhinandhan Narayanan, Kalyan K. Srinivasan**, Sundar R. Krishnan****

* Dept. of Industrial Engineering - University of Bologna
** Dept. of Mechanical Engineering, The University of Alabama, Tuscaloosa

Corresponding author's e-mail: giacomo.silvagni2@unibo.it

Abstract. In the field of internal combustion engines, the Low Temperature Combustions (LTC) appear to have the potential to reduce the formation of both soot and nitrogen oxides. One of the most promising LTC is Reactivity Controlled Compression Ignition (RCCI) which is based on the combustion of a lean low reactivity fuel-air mixture generated in the intake manifold and autoignited by small injections of high reactivity fuel introduced at high pressure in the combustion chamber. By the combination of net-zero natural gas and biodiesel, such LTC methodology might represent a suitable solution moving toward zero-emissions in transportation sector.
Despite the potential to reduce pollutant emissions, Low Temperature Combustion strategies face a challenge in controlling the angular position where the combustion takes place which can be overcome by a proper management of the high-pressure injections.
One potentially interesting application is related to trucks, mainly because they have long periods of idling, since emissions can be drastically reduced by means LTC. A single cylinder research engine for heavy duty application is operated under steady state conditions at low load and speed to analyze the possibility of controlling the engine behavior in dual fuel RCCI mode. The results indicate that the combustion mode switches from the dual-stage to gaussian within a narrow angular range. A further advance of the start of injection can generate misfires and significant variations in typical combustion indexes, while a delayed start of injection can cause impulsive combustion that rises the cylinder temperature and results in high-frequency pressure oscillations inside the combustion chamber. These oscillations are related to the combustion chamber typical resonance frequency, and if relevant in amplitude and persist for a long time, they might generate a potential source of failures.

1. Introduction

An analysis conducted by the Environmental Protection Agency (EPA) indicates that heavy-duty vehicles (HDV) significantly contribute to global emissions within the transportation sector [1, 2]. Of particular concern is the impact during idling, as drivers often keep the trucks idle for extended periods due to reasons such as waiting for deliveries, border crossings, loading/unloading goods, and adhering to rest periods. To ensure driver comfort during these phases the engine have to generate power for heating, ventilation, air conditioning, and other onboard systems.

In response to the negative environmental consequences of idling, several districts in North America are implementing regulations to limit truck idling time. As part of global decarbonization efforts, the use of biofuels combined with advanced combustion strategies, such Low Temperature Combustions (LTC), along with effective cycle-based control mechanisms, are considered suitable solutions to meet increasingly stringent emissions regulations for internal combustion engines. Numerous research centers have conducted experiments to demonstrate the effectiveness of various combustion strategies, including pre-chamber combustion [3, 4], Homogeneous Charge Compression Ignition (HCCI) [5, 6], and Reactivity Controlled Compression Ignition (RCCI) [7-12]. These strategies, combined with innovative methodologies and low-cost sensors for cylinder-to-cylinder combustion phase control [13-15], have exhibited high fuel conversion efficiencies and low emissions [16-24].

Given these circumstances, a research initiative has been conducted by a collaboration between the University of Alabama and the University of Bologna aimed at exploring the potential of an ultra-low emissions combustion methodology, the Reactivity Controlled Compression Ignition (RCCI), during idling engine conditions in a heavy-duty single cylinder research engine [25, 26]. The target of the study was to find a viable alternative overcoming the well-known limitation of standard diesel combustion in terms of emissions, efficiency, and control.

However, one of the challenges associated with implementing RCCI technology is managing combustion within a narrow range where optimal efficiency, emissions, repeatability, and stability can be achieved. This paper presents an analysis based on experimental activity conducted at the Combustion Lab of the University of Alabama running a single cylinder research engine operated in RCCI dual-fuel combustion mode at low load.

The study focuses on analyzing combustion behavior using a pressure sensor in the combustion chamber while varying the start of the angular position of the high reactivity fuel injection (SOI). Depending on the SOI position, combustion occurs with different characteristics. By the analysis of the power spectrum of the in-cylinder pressure signal, the magnitude of resonant frequencies of the combustion chamber, determined by the impulsivity of the combustion process, were observed and analyzed. A deep knowledge of such oscillatory phenomenon is crucial to preserve the engine from critical damage on structural components and auxiliaries when very impulsive combustion occurs.

2. Experimental Set-Up

The experimental activity was conducted on a single-cylinder PACCAR MX11 engine (specifications in Table 1), operating at a constant rotational speed using a 393 HP AC dynamometer and a Dyne Systems IL5 controller. A common rail direct injection system was employed to inject the High Reactivity Fuel (HRF) in the combustion chamber. The pressure control and the injection management were demanded to National Instruments DCM device interfaced with Vieletech's Calibration Viewer software. The Low Reactivity Fuel (LRF) was introduced into the intake manifold, and its flow was regulated using a Swagelok KLF series pressure regulator. Both fuel flows rates were measured using Emerson Micromotion Coriolis flowmeters.

Fresh air was supplied to the intake manifold through an external compressor, decoupled from the engine, using a calibrated orifice operating under sonic block conditions. The air flow was then regulated by controlling the pressure and temperature upstream of the orifice, measured using a Setra 206S pressure transducer and an Omega K-type thermocouple, respectively.

The in-cylinder pressure was measured using a Kistler piezoelectric pressure transducer (6124A) coupled with a charge amplifier (type 5018). The angular synchronization of the in-cylinder pressure signal was performed through BEI encoder with 0.1 crank angle degree (CAD) resolution. Furthermore, two Kistler piezoresistive pressure transducers were used to monitor the pressure dynamics of both the intake and exhaust systems.

Table 1. Engine specifications

Engine type	*Single cylinder, four-stroke*
Displaced volume	*1806 cm^3*
Maximum Torque	*350 Nm @ 1000 rpm*
Maximum Power	*53 kW @ 1750 rpm*
Injection System	*Common Rail Injection system*
Bore	*123 mm*
Stroke	*152 mm*
Compression ratio	*18.5:1*
Intake Valve	*IVO: 350° aTDC*
	IVC: -150° aTDC
Exhaust Valve	*EVO: 130° aTDC*
	EVC: -355° aTDC
Maximum Speed	*2200 rpm*
Maximum Pressure	*245 bar*

3. Combustion transition analysis

To simulate a typical idle condition, the tests were carried out at low load and 1339 rpm. With the aim of analyzing the impact of HRF injection position on the combustion behavior, different Start of Injection (SOI) values were chosen.
In the following Table 2 the principal test condition data are summarized.

Table 2. Engine test conditions

Engine speed [rpm]	Intake manifold pressure [bar]	Diesel fuel injection pressure [bar]	Intake Temperature [°C]	HRF SOI [° aTDC]
1341	1.48	500	20	-50
1337	1.48	500	20	-45
1337	1.48	500	20	-40
1340	1.48	500	20	-35
1340	1.48	500	20	-30
1338	1.48	500	20	-25
1338	1.48	500	20	-20
1338	1.48	500	20	-15
1338	1.48	500	20	-10

To highlight the typical combustion phase trends of RCCI combustion, the following figures report the pressure traces in a wide angular range around the top dead center during the SOI sweep described in Table 2. A distinct color is used to track the trends of the quantities of interest, along with the angular range where the HRF is injected. The sampling rate of the pressure signal is 200 kHz, and the following figures present the data low pass filtered at 20 kHz after their conversion in the angular domain.

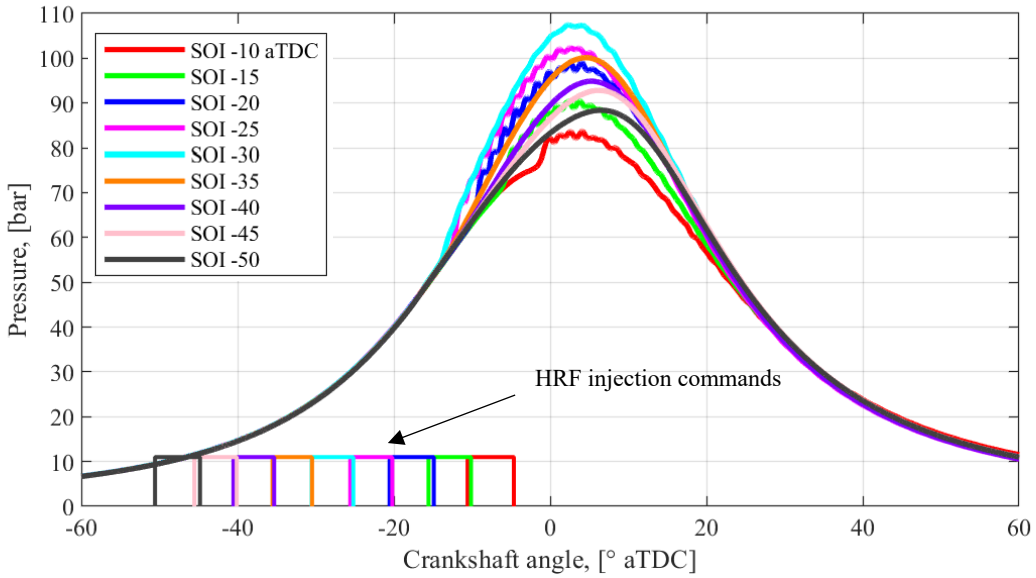

Figure 1. Pressure trends at different SOI values, from -50° to -10° aTDC

By looking at Figure 1 it can be seen that moving the SOI from -50° up to -15° aTDC, despite the very different SOI values of the high reactivity fuel injection, at first glance no differences are visible respect the pressure trends and they follow the same compression curve. The same consideration can be done regarding the trend of the mean temperature inside the cylinder, shown in Figure 2.
Comparing the different trends in both Figures 1 and 2, it can be noticed the presence of a high frequency oscillation for the retarded SOIs (from -30 to -10° aTDC), while for the advanced SOIs (from -50 to -35° aTDC) both pressure and temperature trends are smoothly.

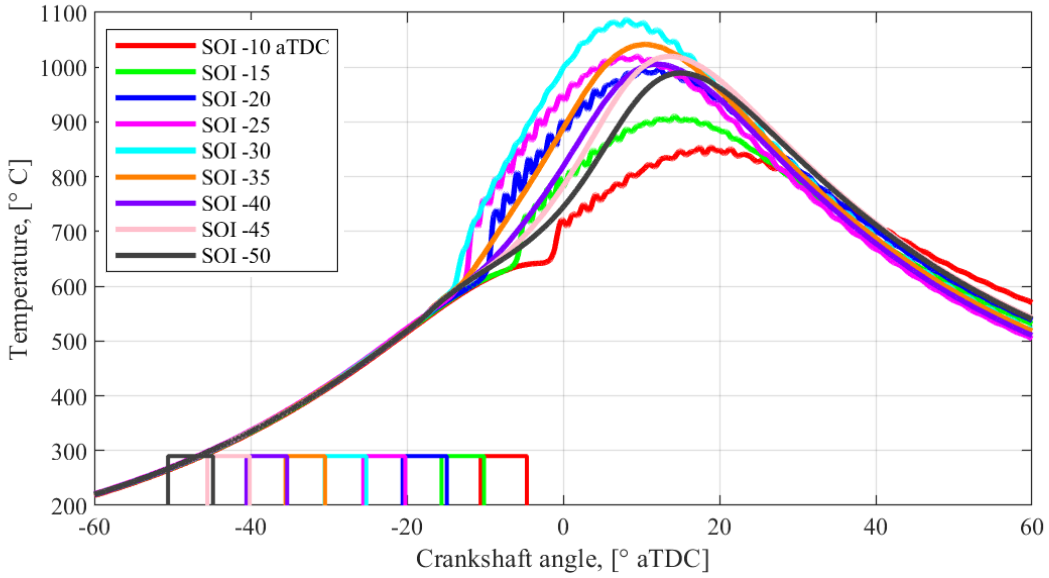

Figure 2. Temperature traces at different SOI values, from -50° to -10° aTDC

From the analysis of figures 1 and 2 it can be stated that since the angular SOI position of the HRF injection range from -50° to -10° aTDC, the thermodynamic conditions in correspondence of the fuel injection angle are quite different. As a matter of fact, in such conditions the pressure and temperature changes from 10 to 60 bar and from 260° C to about 600° C respectively.
To have a better understanding of the combustion behavior, the derivative of the cylinder pressures were evaluated, as shown in figure 3. To improve the readability of the pressure derivative trends, the comparison shown in Figure 3 was performed limiting the pressure derivative values to 5 bar/°. As a result, the SOI -30, -25, -20, -15 and -10° aTDC pressure derivative traces were interrupted.

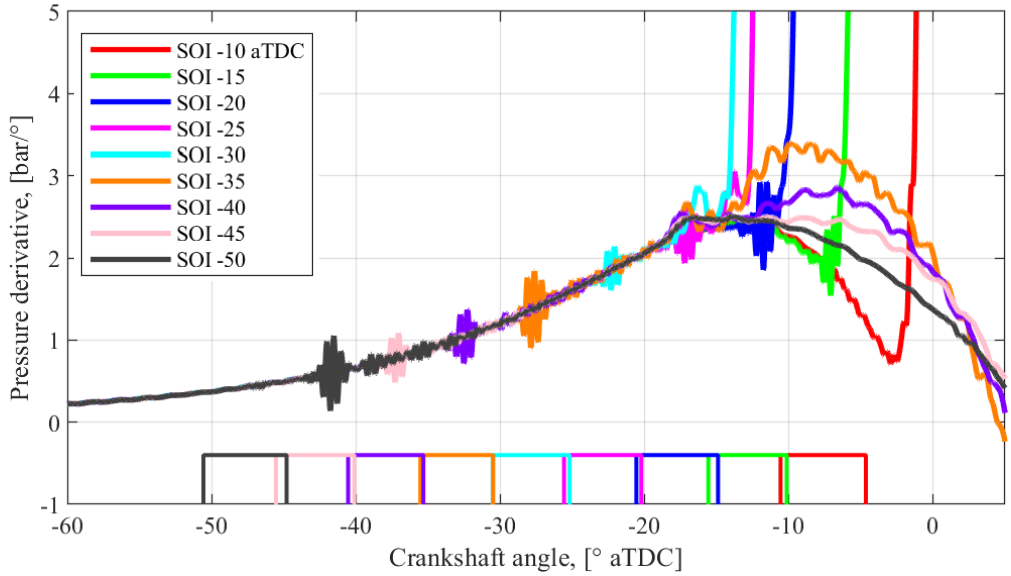

Figure 3. Pressure derivative at different SOI values, from -50° to -10° aTDC

The derivative trends presented in Figure 3 are interesting because they show a high frequency oscillation in an angular range of 2-3° about 9° after the SOI. (except for the last SOI value at -10° aTDC). Since no significative variation in pressure and temperature were observed where these oscillations are present, it can be stated that they are mechanical vibrations due to the injector closure.
To have a better understanding of the combustion process, according to the well-known Equation 1, the Rate of Heat Release (RoHR) was evaluated staring from the pressure traces, shown in Figure 4.

$$RoHR = \frac{1}{\gamma - 1}\left(V\frac{dp}{d\theta} + \gamma\, p\frac{dV}{d\theta}\right) \quad (1)$$

Before performing the RoHR evaluation, the pressure traces were low pass filtered at 4 kHz. Such process decreases the high frequency content of the signal allowing an easier comparison between the different combustion behaviors. Figure 4 reports the comparison of RoHR traces during the SOI sweep running the engine in RCCI mode. From the analysis of Figure 4, it can be seen that the RoHR traces are similar each other in the angular range from -50° up to -20° aTDC, while after this latter angular position the trends are clearly different, meaning that the combustion processes change their characteristics.

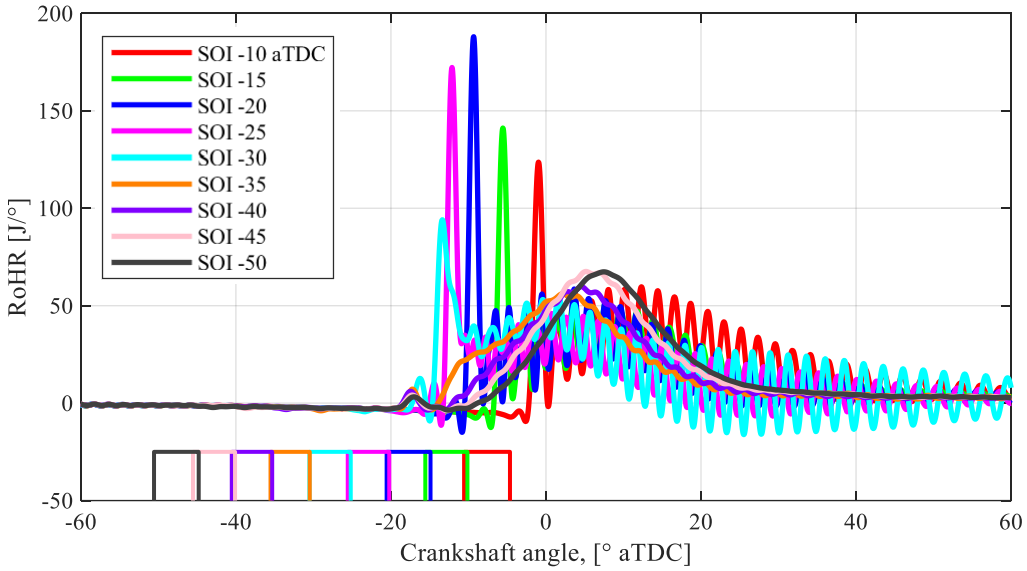

Figure 4. Rate of heat release at different SOI values, from -50° to -10° aTDC

From Figure 4 it can be seen that the combustion changes mode from Gaussian, when the SOI of the high reactivity fuel is very advanced, to dual-stage, when the SOI is retarded. To better distinguish the behavior of the combustion during the SOI sweep, Figure 5 reports the RoHR with the trend interrupted when the RoHR exceed the value of 80 J/°.

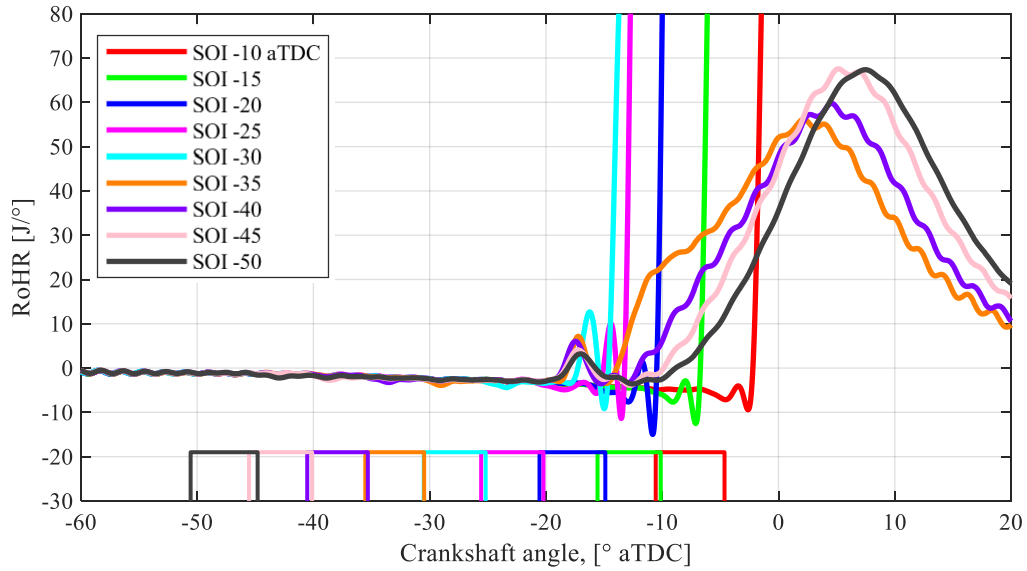

Figure 5. Rate of heat release at different SOI values, from -50° to -10° aTDC, with the trend interrupted when the RoHR exceed the value of 80 J/°

In particular, the changes in the combustion mode take place for SOI from -35° to -30° aTDC. To better highlight the transition from a Gaussian to dual-stage combustion, Figure 6 shows only two RoHR trends: SOI -35° (Gaussian combustion) and -30° aTDC (dual-stage combustion) respectively. The RoHR trace related to SOI -30° aTDC clearly shows the presence of the premixed combustion,

followed by a smoother second combustion stage, while the trend for SOI value of -35° aTDC shows only a progressive single combustion.

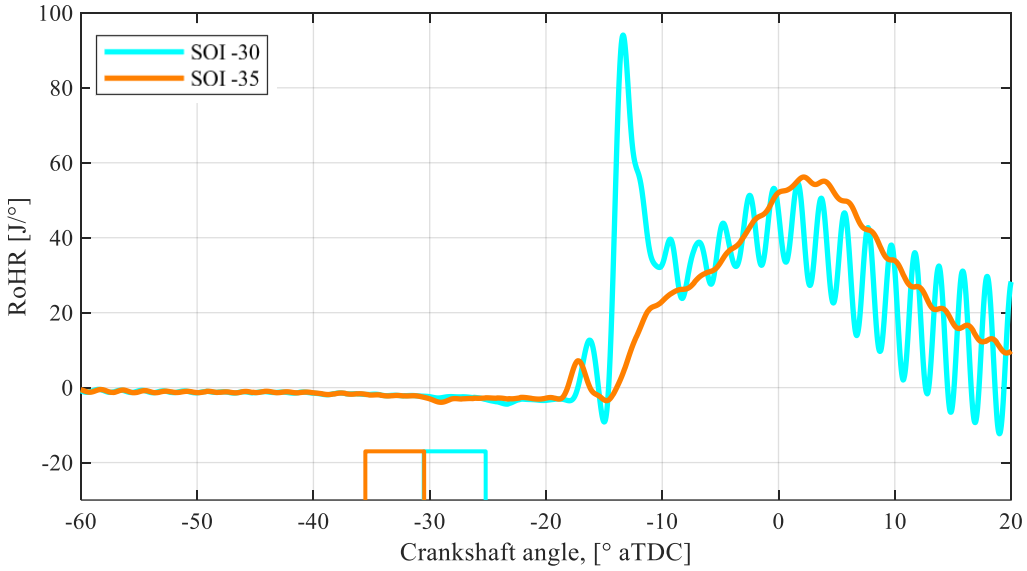

Figure 6. Rate of Heat release for different SOI values -35° and -30° aTDC

To highlight the change in the combustion mode in the following Figures the RoHR trends are presented separately: in Figure 7 the ones which are characterized by a gaussian combustion, with SOI ranging from -50° to -35° aTDC while in Figure 8 the ones performing a double stage combustion, with SOI ranging from -30° to -10° aTDC. To better recognize the different phenomenon occurring between the start of the fuel injection and the start of the combustion, such Figures present RoHR values within the range -18 to 13 of J/°.

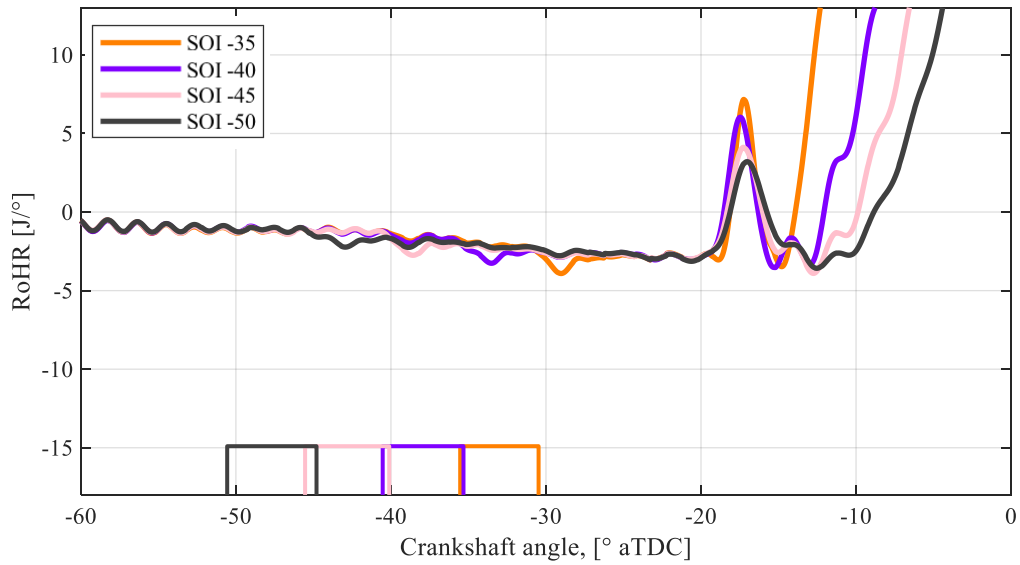

Figure 7. Rate of Heat release in the starting phase of the combustion at different SOI values, from -50° to -35° aTDC

From Figure 7 it can be clearly noticed that a first combustion occurs for all the SOI from -50° to -35° aTDC in the range from -19° to -15.5° aTDC: overall, all the RoHR traces present their maximum value at about -17.5° aTDC. Such phenomenon, named as Low Temperature Heat Release (LTHR) is extremely common when a LTC methodology characterized by spontaneous ignition is analyzed. Several works in the field of LTC demonstrated the link between LTHR and LTC, especially RCCI. The presence and the intensity of the LTHR can be related to the air-fuel mixture chemistry and thermodynamic conditions under which the combustion takes place. It can also be observed that the more advanced is the SOI, the lower is the maximum value of LTHR. After the LTHR, the main combustion takes place (Gaussian) with the pressure derivative slightly increasing moving from SOI -50° to -35° without exceeding 3.5 bar/° and with a correspondent RoHR maximum value under 70 J/°.

The change in SOI from -35° to -30° aTDC causes a sudden variation of the combustion behavior that can be analyzed considering Figure 4 and Figure 8: the more retarded fuel injection position (SOI -30° aTDC) moves the angular range of the LTHR between -18° and -15° aTDC with the maximum value of 12 J/° at -16° aTDC. The combustion process moves on with the premixed phase characterized by a pressure derivative and RoHR values significantly higher in comparison with the previous analyzed Gaussian combustion.

In these latter (Retarded SOIs), the premixed combustion stage occurs with a violent release of heat that is responsible of the high frequency oscillation that affects the pressure trend immediately after the first combustion stage, Figures 4 and Figure 6.

Moreover, from Figure 8 it can be seen that for SOI from -25° to -10° aTDC the LTHR tends to disappear but the energy release starts with the first combustion stage with a high maximum value of RoHR over 90 J/°. The angular delay between the SOI and the effective premixed combustion decreases as the SOI is retarded because the cylinder temperature increases from 460° C to 600° C and cylinder pressure from -30 to -60 bar: for SOI -25° aTDC the angular delay between SOI and SOC can be evaluated of about 12° while for SOI -10° aTDC it worth 8°.

From Figures 4, 7 and 8 it can also be noticed that the RoHR trend for all the different SOI values before the angular position where the combustion begin are overlapped presenting a declining trend due to the heat losses toward the cylinder wall.

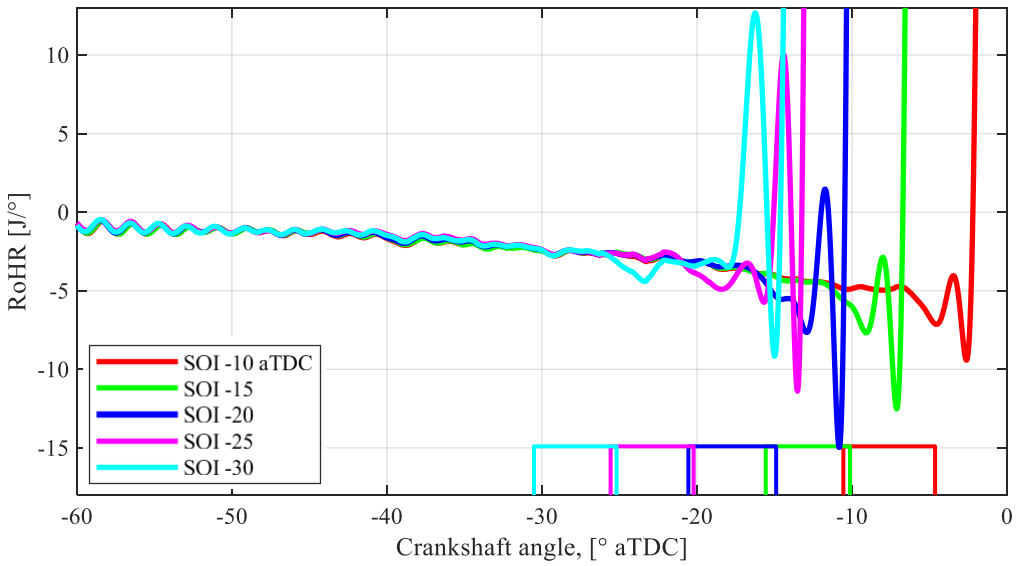

Figure 8. Rate of Heat release in the starting phase of the combustion at different SOI values, from -30° to -10° aTDC

4. Pressure vibrational analysis

To confirm the different vibrational behavior of the dual stage combustion respect to the Gaussian, the frequencies analysis of the pressure trends was performed. Figure 9 presents the complete frequency range of the pressures signal during the SOI sweep. The color of each trend is related to a specific SOI, as reported in the legend and in the same order like in all the previous figures.

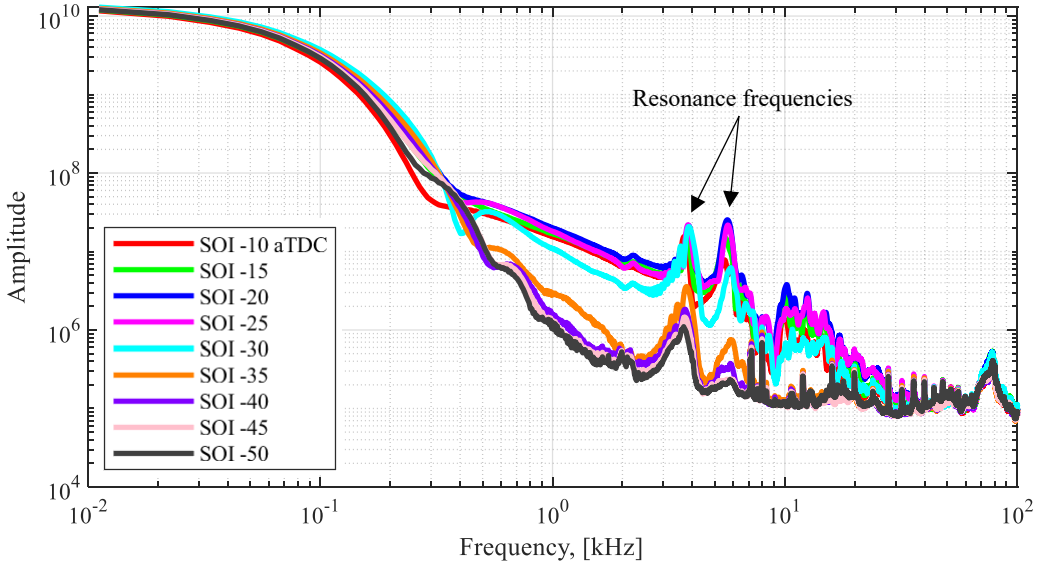

Figure 9. Frequency analysis of the pressures for different SOI values

From Figure 9 it can be seen that the frequency content is almost equal up to 300 Hz for the nine signals, then the trends can be separated in two different groups. The first is composed by SOI -50° to -35° aTDC with a lower frequency amplitude in a frequency range from 300 Hz up to 30 kHz respect the second group composed by SOI -30° to -10° aTDC.

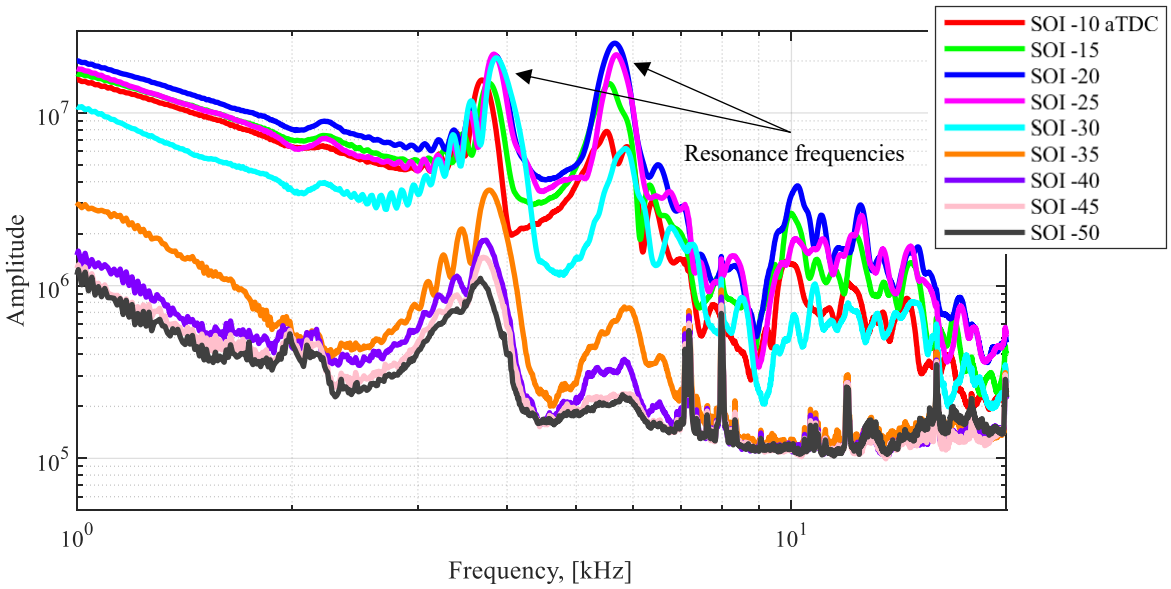

Figure 10. Frequency analysis of the pressures for different SOI values

To better highlight the differences in the frequency domain, in Figure 10 the frequency range from 1 to 20 kHz has been highlighted. Moreover, two frequencies linked to the resonance frequency of the combustion chamber are clearly visible: at 3.8 kHz and at 5.6 kHz. It can also be noticed that the first resonance frequency values present a variation form 3.8 kHz to about 2 kHz. Since it is known that the resonance frequency is temperature dependent by means its square root, the spread reported in Figure 10 can be easily explained by different gas temperatures in the cylinder, which decreases from 1000° C to 500° C. In the cases of SOI from -10° to -30° aTDC the amplitude of the resonance frequency are very close to the reliability limitation of the engine in term of maximum pressure.
Several authors observed different resonance frequencies testing different geometric characteristics of the combustion chamber and thermodynamic conditions of the air-fuel mixture determining the correlation between the frequency and the temperature of the gas for each single mode of vibration [27-29]. The link that Eng [28] found is expressed by Equation 2.

$$f(m,n) = \alpha(m,n)\frac{\sqrt{\gamma RT}}{\pi D} \tag{2}$$

In Equation 2, $f(m,n)$ is the resonance frequency for the m, n vibration mode, $\alpha(m,n)$ the wave number evaluated through Bessel functions, m and n indicate the circumferential and radial pressure nodes, γ is the specific heats ratio, R the ideal gas constant, T the temperature of the gas in the cylinder combustion chamber, and D is the cylinder diameter. The lowest frequency mode is the circumferential one, with m=1 and n=0, and its frequency value evaluated at T=900° C is about 5.5 kHz. In Figure 11 some of the vibrational modes of a cylinder are presented: the first four are radial modes while the last is circumferential.

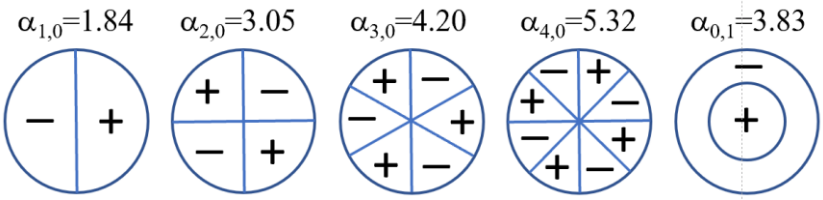

Figure 11. Vibration modes of a cylindrical combustion chamber

Due to the intake and exhaust valve closing against their seat and to the closure of the fuel injector, the frequency content in the frequency range 15 kHz - 25 kHz is correlated with the impact, the latter clearly visible in Figure 3 at about 8° after the respective SOI of the high reactivity fuel.

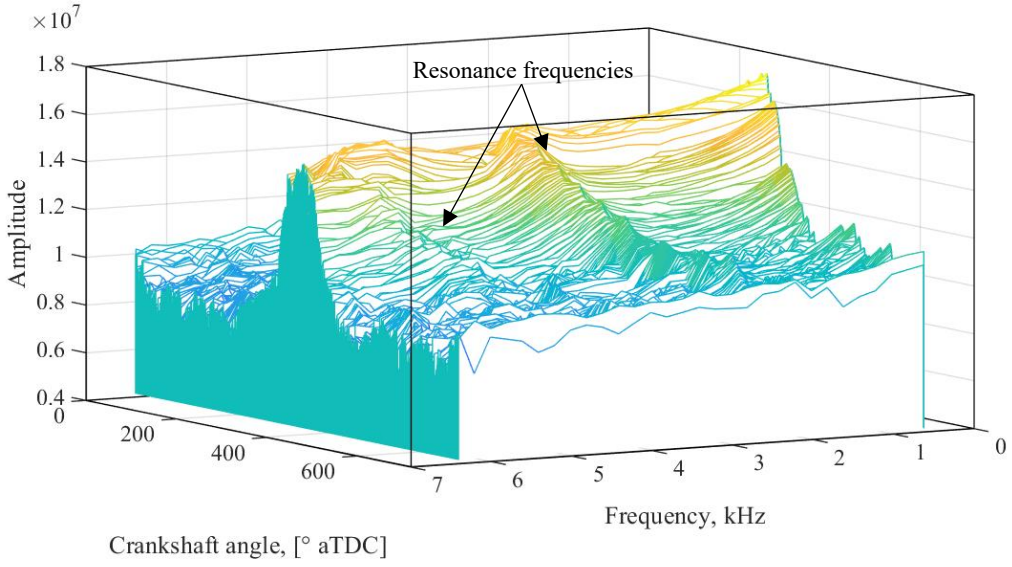

Figure 12. Time-frequency analysis of a pressure cycle with high reactivity fuel SOI at -20° aTDC

As an example, to confirm the dependence of the first resonance frequency from the temperature a time-frequency analysis of the pressure trend with SOI -20° aTDC is presented in Figure 12.
In Figure 12, the time axis was replaced with the crank angle axis because it allows to associate the resonance frequency of the combustion chamber with the angular reference of the cycle.
It can be observed that near the top dead center the start of the combustion, due to its impulsiveness, excites the entire pressure signal frequency range.
After the start of the combustion a clearly visible ridge on the left side of the surface is present, starting at 4 kHz around the angular position of 400°. It subsequently develops throughout the remaining part of the cycle with a progressive decrease in frequency value. However, it still maintains with an amplitude value that allows it to be distinguished from the general noise of the other frequencies.
In Figure 13 it is shown the time frequency related to a pressure cycle with SOI at -50° aTDC, characterized by a Gaussian combustion shape (the amplitude of the first resonance frequency is significantly lower).

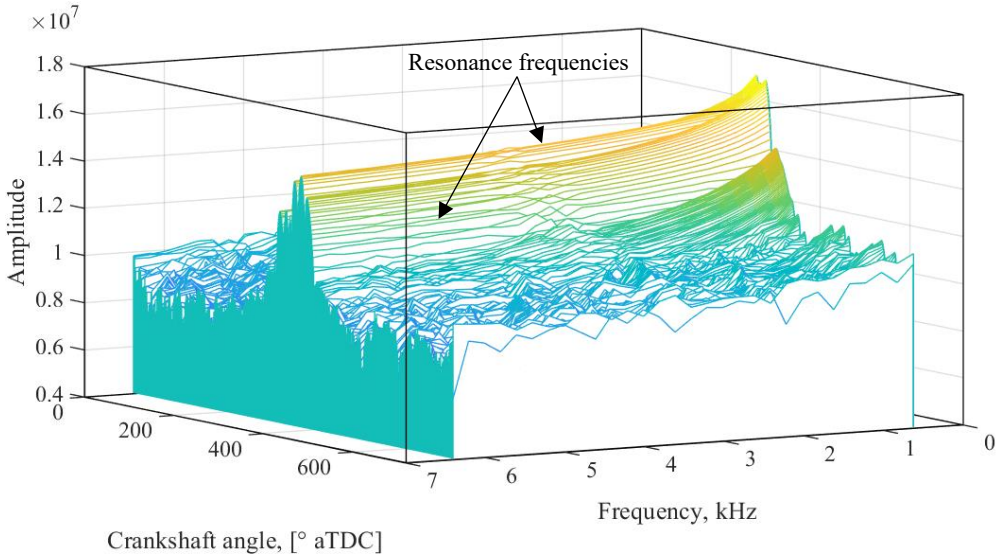

Figure 13. Time-frequency analysis of a pressure cycle with high reactivity fuel SOI at -50° aTDC

By comparing Figure 13 with Figure 12 it can be observed that in the latter case the presence of the ridge associated with the variation of the resonance frequency of the combustion chamber is almost imperceptible. In fact, referring to Figure 10 where the frequency analysis of all the pressure trends as a function of the SOI are reported, the value of its amplitude is an order of magnitude lower than that of the case represented in Figure 12.
In Figure 14 and Figure 15 the clouds related to different SOI are presented. From the analysis of the latter two Figures, it can be observed that moving from SOI -10° to -50°aTDC, the point distributions tend to exhibit a greater dispersion, indicating a decrease in repeatability while the engine is running in a steady state condition. This situation highlights that the running condition of the engine becomes more instable overcoming the misfire threshold as the SOI of the high reactivity fuel is advanced.

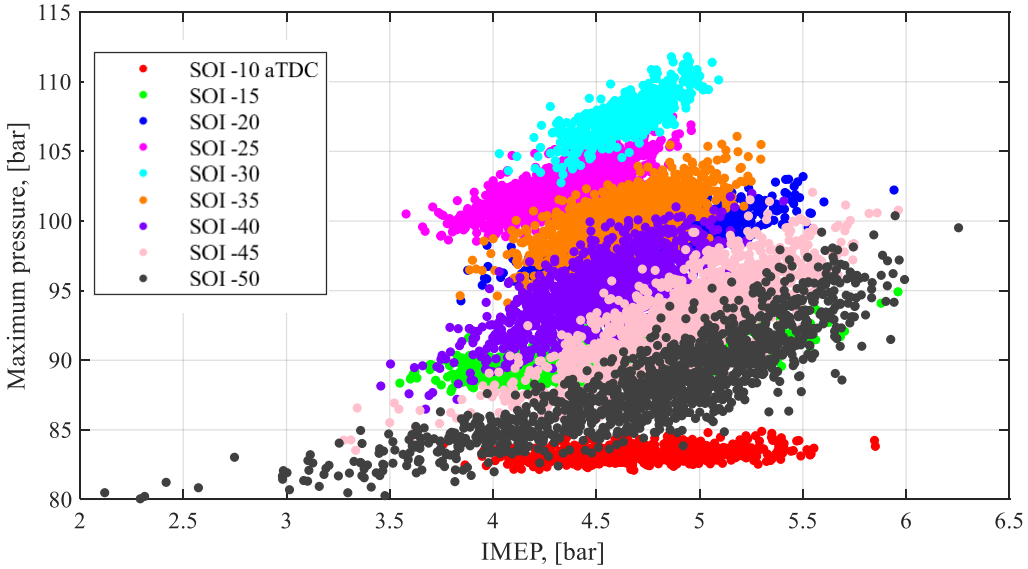

Figure 14. Maximum pressure versus indicated mean effective pressure for different SOI conditions

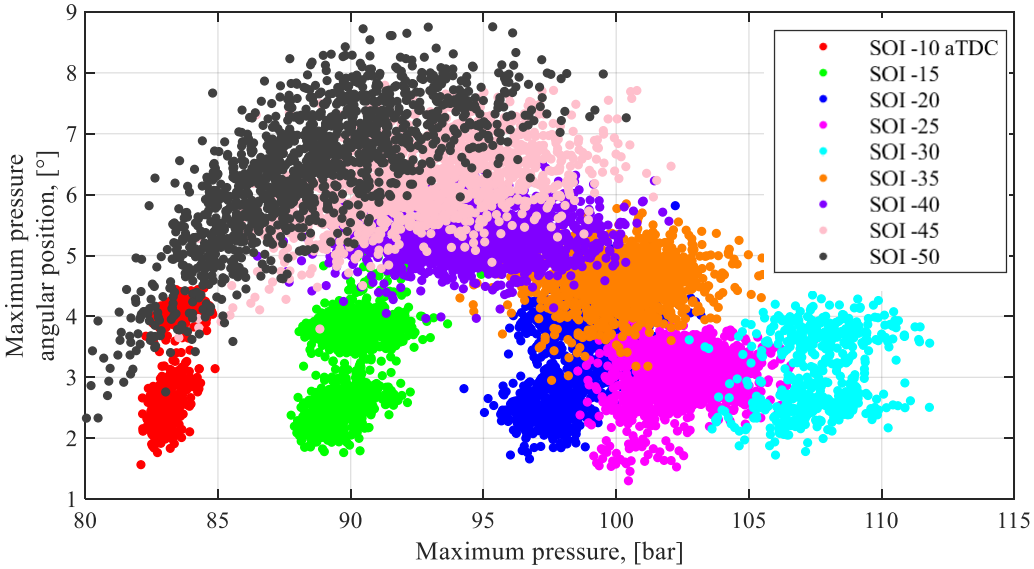

Figure 15. Maximum pressure angular position versus maximum pressure for different SOI conditions

5. Conclusion

The data analyzed allowed to verify that in the dual fuel engine, where a low reactivity fuel-air mixture is ignited by the injection of a high reactivity fuel, the combustion behavior is very sensitive to the SOI, passing from a dual stage combustion if the SOI is retarded to a gaussian mode when the SOI is advanced. In the first limiting case, the presence of a very impulsive first combustion stage, that involves a significant amount of fuel within the combustion chamber resulting in a violent release of energy, promotes the propagation of pressure waves that increase the loads acting on the piston and the operational noise of the engine itself. The time frequency analysis confirms the presence of the pressure propagation inside the cylinder whose frequency is linked to the temperature of the exhaust gas inside the combustion chamber.

In the second case, the combustion exhibits a smother shape, but its combustion indices are characterized by a remarkable cyclic variations, which can even lead to misfires.
As previously mentioned, it is possible to identify a narrow range of SOI values that provide the best compromise in terms of engine behavior repeatability, without exciting resonance frequency whose amplitudes that could potentially lead to long-term damage to the engine components.
Future research will be conducted to better understand the impact of each engine control parameter on the combustion phase and the ignition stage. Such analysis will be achieved by estimating the cycle-to-cycle time delay between the Start of Injection and Start of Combustion of the high reactivity fuel, to define the proper Start of Injection position of the pilot injections. This will ensure that the Start of Combustion of the low reactivity fuel is within the desired angular range, thus guaranteeing a gaussian combustion with high efficiency and low pollutants.

References

[1] EPA, “Motor Coach Idling Field Observation Study for Washington, DC, Metro Area”, US Environmental Protection Agency, Washinton, DC, USA, 2006, Report EPA420-S-06-2006
[2] Lim, H., “Study of Exhaust Emissions From Idling Heavy-Duty Diesel Trucks and Commercially Available Idle-Reducing Devices”, 2003, SAE Technical Paper 2003-01-0288, DOI: 10.4271/2003-01-0288
[3] J. Shin, J. Choi, J. Seo, S. Park, “Pre-chamber combustion system for heavy-duty engines for operating dual fuel and diesel modes”, Energy Convers Manag, 255 (2022), DOI: 10.1016/j.enconman.2022.115365
[4] M.M. Salahi, V. Esfahanian, A. Gharehghani, M. Mirsalim, “Investigating the reactivity controlled compression ignition (RCCI) combustion strategy in a natural gas/diesel fueled engine with a pre-chamber”, Energy Convers Manage, 132 (2017), DOI: 10.1016/j.enconman.2016.11.019
[5] Thring R. “Homogeneous-Charge Compression-Ignition (HCCI) engines”, SAE technical paper 892068, 1989, DOI: 10.4271/892068
[6] Christensen M, Johansson B., “Supercharged homogeneous charge compression ignition (HCCI) with exhaust gas recirculation and pilot fuel”, SAE technical paper 2000-01-1835, 2000, DOI: 10.4271/2000-01-1835
[7] Kokjohn, S., Hanson, R., Splitter, D., Kaddatz, J., Reitz, R., "Fuel Reactivity Controlled Compression Ignition (RCCI) Combustion in Light- and Heavy-Duty Engines," SAE Int. J. Engines 4(1):360-374, 2011, DOI: 10.4271/2011-01-0357.
[8] Hanson, R., Kokjohn, S., Splitter, D., Reitz, R., "Fuel Effects on Reactivity Controlled Compression Ignition (RCCI) Combustion at Low Load," SAE Int. J. Engines 4(1): 394-411, 2011, DOI: 10.4271/2011-01-0361.
[9] Stola, F., Ravaglioli, V., Silvagni, G., Ponti, F., De Cesare M., "Injection Pattern Investigation for Gasoline Partially Premixed Combustion Analysis", SAE Technical Paper 2019-24-0112, 2019, DOI: 10.4271/2019-24-0112.
[10] Silvagni, G., Narayanan, A., Ravaglioli, V., Srinivasan, K.K., Krishnan, S.R., Collins, N., Puzinauskas, P.; Ponti, F., "Experimental Characterization of Hydrocarbons and Nitrogen Oxides Production in a Heavy-Duty Diesel–Natural Gas Reactivity-Controlled Compression Ignition Engine", Energies 2023, 16, 13, 5164, DOI: 10.3390/en16135164
[11] Narayanan A., Hariharan D., Partridge K., Pearson A., Srinivasan K., Krishnan S., “Impact of Low Reactivity Fuel Type and Energy Substitution on Dual Fuel Combustion at Different Injection Timings”, Energies 2023, 16, 1807, DOI: 10.3390/en16041807
[12] Hariharan D., Partridge K., Narayanan A., Srinivasan K., Krishnan S.R., Anandaraman N., “Strategies for Reduced Engine-Out HC, CO, and NOx Emissions in Diesel-Natural Gas and POMDME-Natural Gas Dual-Fuel Engine”, SAE Int. J. Adv. & Curr. Prac. in Mobility, DOI: 10.4271/2022-01-0460

[13] Businaro A.; Cavina N.; Corti E.; Mancini G.; Moro D.; Ponti F.; Ravaglioli V., "Accelerometer based methodology for combustion parameters estimation", Energy Procedia, Vol. 81, 950-959, 2015, DOI: 10.1016/j.egypro.2015.12.152
[14] V. Ravaglioli, N. Cavina, A. Cerofolini, E. Corti, D. Moro, F. Ponti, "Automotive Turbochargers Power Estimation Based on Speed Fluctuation Analysis", Energy Procedia, Volume 82, 2015, Pages 103-110, ISSN 1876-6102, DOI: 10.1016/j.egypro.2015.11.889
[15] Corti, E., Raggini, L., Rossi, A., Brusa, A., Silvestri, N., Cucchi, M., "Application of Low-Cost Transducers for Indirect In-Cylinder Pressure Measurements", *SAE Int. J. Engines* 16(2):213-230, 2023, DOI: 10.4271/03-16-02-0013
[16] A. Paykani, A. Garcia, M. Shahbakhti, P. Rahnama, R.D. Reitz, "Reactivity controlled compression ignition engine: Pathways towards commercial viability", Appl Energy, 282 (2021), Article 116174, DOI: 10.1016/j.apenergy.2020.116174.
[17] J. Benajes, A. García, J. Monsalve-Serrano, D. Villalta, "Fuel consumption and engine-out emissions estimations of a light-duty engine running in dual-mode RCCI/CDC with different fuels and driving cycles", Energy Convers Manage, 157 (2018), pp. 277-287, DOI: 10.1016/J.ENERGY.2018.05.144
[18] Silvagni, G.; Ravaglioli, V.; Falfari, S.; Ponti, F.; Mariani, V., "Development of a Control-Oriented Ignition Delay Model for GCI Combustion", Energies 2022, 15, 6470. DOI: 10.3390/en15176470
[19] A. Kakaee, P. Rahnama, A. Paykani, "Numerical Study of Reactivity Controlled Compression Ignition (RCCI) Combustion in a Heavy-Duty Diesel Engine Using 3D-CFD Coupled with Chemical Kinetics", International Journal of Automotive Engineering., 4 (2014), pp. 792-804
[20] R.D. Reitz, G. Duraisamy, "Review of high efficiency and clean reactivity controlled compression ignition (RCCI) combustion in internal combustion engines", Prog Energy Combust Sci, 46 (2015), pp. 12-71, DOI: 10.1016/j.pecs.2014.05.003
[21] Krishnan, S. R., Srinivasan, K. K., Singh, S., Bell, S. R., Midkiff, K. C., Gong, W., Fiveland , S. B., and Willi, M. , "The advanced injection Low Pilot Ignited Natural Gas engine: A combustion analysis", ASME. J. Eng. Gas Turbines Power. July 2004; 126(3), DOI: 10.1115/1.1915428
[22] Ravaglioli, V., Ponti, F., Silvagni, G., Moro, D. et al., "Investigation of Gasoline Partially Premixed Combustion with External Exhaust Gas Recirculation," SAE Int. J. Engines 15(5):613-629, 2022, DOI: 10.4271/03-15-05-0033
[23] Raihan, MS, Guerry, ES, Dwivedi, U, Srinivasan, KK, Krishnan, SR., "Experimental analysis of diesel-ignited methane dual-fuel low-temperature combustion in a single-cylinder diesel engine", J Energ Eng 2015; 141(2): C4014007, DOI: 10.1061/(ASCE)EY.1943-7897.0000235.
[24] Krishnan, SR, Srinivasan, KK, Raihan, MS, "The effect of injection parameters and boost pressure on diesel-propane dual fuel low temperature combustion in a single-cylinder research engine", Fuel 2016; 184: 490–502, DOI: 10.1016/j.fuel.2016.07.042
[25] Raihan, MS, Guerry, ES, Dwivedi, U, Srinivasan, KK, Krishnan, SR. "Experimental analysis of diesel-ignited methane dual fuel low temperature combustion in a single cylinder diesel engine", J Energ Eng 2014; 141(2), C4014007, DOI: 10.1061/(ASCE)EY.1943-7897.0000235
[26] Krishnan, SR, Srinivasan, KK, Raihan, MS, "The effect of injection parameters and boost pressure on diesel-propane dual fuel low temperature combustion in a single-cylinder research engine", Fuel 2016; 184: 490–502, DOI: 10.1016/j.fuel.2016.07.042
[27] Scholl D., Davis C., Russ S., Barash T., "The Volume Acoustic Modes of Spark-Ignited Internal Combustion Chambers", SAE paper 980893, DOI: 10.4271/980893
[28] Eng J.A., "Characterization of pressure waves in HCCI combustion", SAE paper 2002-01-2859, DOI: 10.4271/2002-01-2859
[29] Dahl D., Andersson M., Denbratt I., "The Origin of Pressure Waves in High Load HCCI Combustion: A High-Speed Video Analysis", Combustion Science and Technology, 183:11, 1266-1281, DOI: 10.1080/00102202.2011.589875